# Number-phase minimum-uncertainty state with reduced number uncertainty in a Kerr nonlinear interferometer

M. Kitagawa and Y. Yamamoto
*Nippon Telegraph and Telephone Corporation (NTT) Electrical Communications Laboratories, 3-9-11 Midori-cho, Musashino-shi, Tokyo 180, Japan*
(Received 14 April 1986)

The output state of a nonlinear Mach-Zehnder interferometer is shown to be an effective number-phase minimum-uncertainty state with reduced photon-number uncertainty. This interferometer includes an optical Kerr medium in one arm with a coherent-state input. Unusual "crescent"-shaped squeezing which preserves photon number is revealed in the unitary evolution associated with a self-phase-modulation in the Kerr medium. Photon-number uncertainty $\langle \Delta\hat{n}^2 \rangle$ can be reduced by interference with a coherent-state reference wave. It can be minimized to $\langle \hat{n} \rangle^{1/3}$, far below the limit $\langle \hat{n} \rangle^{2/3}$ achieved by an ordinary squeezed state. The increased phase uncertainty due to self-phase-modulation and the reduced photon-number uncertainty still preserve the minimum-uncertainty product $\langle \Delta\hat{n}^2 \rangle \langle \Delta\hat{\Phi}^2 \rangle \sim \frac{1}{4}$.

## I. INTRODUCTION

Considerable interest has recently been focused on novel photon states without classical analog. Ordinary squeezed states in particular have been intensively studied.[1,2] Such squeezed states feature different uncertainties in two quadrature amplitudes, $\hat{a}_1$ and $\hat{a}_2$. Their product still satisfies the minimum value allowed by the Heisenberg uncertainty relation $\langle \Delta\hat{a}_1^2 \rangle \langle \Delta\hat{a}_2^2 \rangle = \frac{1}{16}$. Squeezed states are a generalization of Glauber's coherent state[3] with $\langle \Delta\hat{a}_1^2 \rangle = \langle \Delta\hat{a}_2^2 \rangle = \frac{1}{4}$ directed toward the eigenstates of $\hat{a}_1$ or $\hat{a}_2$.[4] Extensive experimental efforts[5-10] have been devoted to the realization of squeezed states based on four-wave-mixing schemes.[11-15] Phase-sensitive noise, a precursor of squeezing, has recently been observed in the classical region.[8,10] Slusher *et al.* have observed the generation of these ordinary squeezed states.[9]

Another kind of nonclassical photon state has been predicted. It is referred to as the amplitude-squeezed state.[16] The amplitude-squeezed state features a reduced photon-number uncertainty $\langle \Delta\hat{n}^2 \rangle < \langle \hat{n} \rangle$ and an enhanced phase uncertainty $\langle \Delta\hat{\Phi}^2 \rangle > 1/4\langle \hat{n} \rangle$. The product of these two uncertainties satisfies the other minimum-uncertainty relation, $\langle \Delta\hat{n}^2 \rangle \langle \Delta\hat{\Phi}^2 \rangle \sim \frac{1}{4}$. This is another generalization of coherent state with $\langle \Delta\hat{n}^2 \rangle = \langle \hat{n} \rangle$ and $\langle \Delta\hat{\Phi}^2 \rangle \sim 1/4\langle \hat{n} \rangle$ (Ref. 17) directed toward the photon-number eigenstate. A reduced photon-number uncertainty will contribute to various kinds of nonclassical behavior; noise reduction below the shot-noise level in direct detection, sub-Poissonian statistics in photon counting, and photon antibunching in a Hanbury Brown—Twiss type of (intensity-correlation) experiment. Such a state can easily be confused with an ordinary squeezed state in which squeezing is realized along the direction of the coherent excitation. Although the latter also possesses reduced photon-number uncertainty, it is restricted by $\langle \Delta\hat{n}^2 \rangle \geq \langle \hat{n} \rangle^{2/3}$.[18] Directions of squeezing are essentially different between these two states, although this difference is small and not clear in the region of weak squeezing.

One possible scheme for amplitude-squeezed-state generation proposed by Yamamoto *et al.*[16] is a combination of quantum nondemolition measurement (QND) of photon number and negative feedback. Sub-Poissonian photoelectron statistics were actually observed in a negative-feedback semiconductor laser with a destructive photon detector.[19] A quantum nondemolition measurement scheme of photon number was proposed using an optical Kerr effect.[20] This scheme may open the closed feedback loop in the above experiment and extract amplitude-squeezed states cut out of it. There have been other measurement-feedback schemes proposed for the generation of light with sub-Poissonian photon statistics.[21,22] The light produced in these schemes is weak and entirely incoherent.

Theoretical difficulties common with such measurement-feedback systems stem from the fact that the state evolution in the measurement process is not sufficiently described within the presently formulated framework of quantum mechanics.[23-25] This is much in contrast with ordinary-squeezed-state generation schemes, in which the state evolves from the coherent state or equivalently from the vacuum state through unitary transformation. The interaction Hamiltonian for this unitary evolution is given by[1]

$$H_I = \hbar[\chi_{\rm NL}(\hat{a}^\dagger)^2 + \chi_{\rm NL}^* \hat{a}^2] \ . \tag{1.1}$$

This paper presents an alternative scheme for generating amplitude-squeezed states. This scheme is based on unitary evolution which can properly be described by quantum mechanics. The scheme is a nonlinear Mach-Zehnder interferometer containing an optical Kerr medium as shown in Fig. 1. This is almost the same scheme as that proposed by Ritze and Bandilla[26] except for certain details. Ritze and Bandilla treated the sufficiently weak output field and demonstrated antibunching and enhanced

 

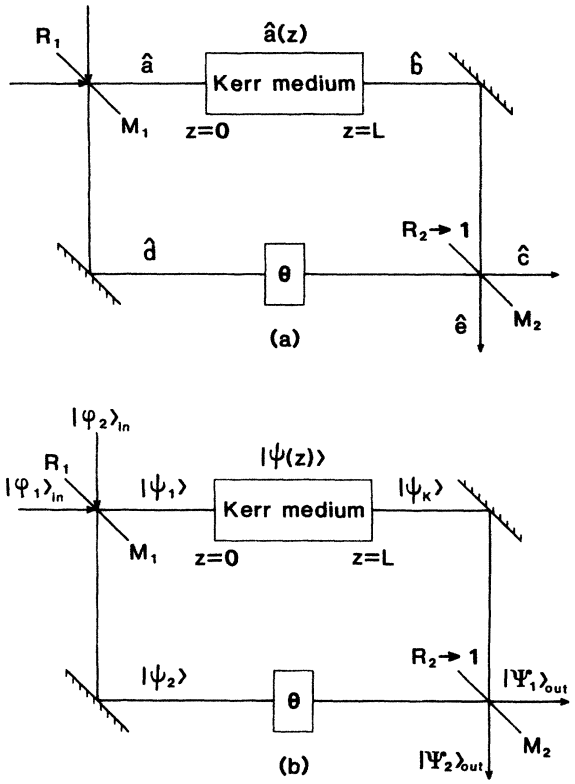


FIG. 1. Nonlinear Mach-Zehnder interferometer with an optical Kerr medium; (a) in the Heisenberg picture; (b) in the Schrödinger picture.

bunching of the output field to be measured in a Hanbury Brown—Twiss type of experiment. We will calculate the quasiprobability density (QPD) (Ref. 27) $\langle \alpha | \rho | \alpha \rangle$ and photon-number distribution $\langle n | \rho | n \rangle$ of the output field and demonstrate that the reduced photon-number uncertainty and enhanced phase uncertainty maintain the minimum-uncertainty product. The interaction Hamiltonian required for this unitary evolution is not as in (1.1) but is given by[28,29]

$$H_I = \hbar \chi_{\rm NL} (\hat{a}^\dagger)^2 \hat{a}^2 . \tag{1.2}$$

The principle of the proposed scheme and a summary of its analysis are presented in Sec. II.

A self-phase-modulation of the single-mode quantized field in the Kerr medium is described in Sec. III based on localized operators.[30] The spatial evolution of the state is demonstrated by QPD in the Schrödinger picture. This evolution corresponds to operator evolution (self-phase-modulation) in the Heisenberg picture.

We show in Sec. IV that photon-number variance can be reduced to $\langle \Delta \hat{n}^2 \rangle = \langle \hat{n} \rangle^{1/3}$. This is far below the limit $\langle \hat{n} \rangle^{2/3}$ for an ordinary squeezed state.[18] The scheme is considered to be a displacement of QPD by interference. Photon statistics exhibit strong sub-Poissonian characteristics even when the mean photon number is relatively small.

Enhanced phase uncertainty and number-phase uncertainty product[31] are discussed in Sec. V. We show that the state prepared using our scheme remains a number-phase minimum-uncertainty state until the maximum reduction of number fluctuation is surpassed.

Section VI discusses the relation between an effective number-phase minimum-uncertainty state generated by our scheme and a mathematically defined minimum-uncertainty state.[32]

## II. PRINCIPLES AND SUMMARY OF ANALYSIS

This paper concerns the nonlinear Mach-Zehnder interferometer containing a Kerr medium in one arm. This is schematically depicted in Fig. 1. Figures 1(a) and 1(b) show the operator evolution in the Heisenberg picture and the state evolution in the Schrödinger picture, respectively. A coherent-state input signal is divided into two parts by the first beam splitter $M_1$. One part $\hat{a}$ propagates along a Kerr medium in which the phase of the signal is modulated by its intensity (photon number) via the self-phase-modulation effect. The other part $\hat{d}$ is not disturbed and is combined with the Kerr-medium output signal $\hat{b}$ by the second beam splitter $M_2$. The interferometer path length difference and the beam splitter $M_2$ phase constant are adjusted so that the two orthogonally oriented signals are combined to form an output signal $\hat{c}$ as shown in Fig. 2. When the intensity of signal $\hat{a}$ increases above its average value, the phase of the Kerr-medium output signal $\hat{b}$ advances and so the combined output-signal intensity is reduced to approach the average value resulting from destructive interference with reference signal $\hat{d}$. When the intensity of signal $\hat{a}$ decreases below its average value, the phase of the Kerr-medium output signal $\hat{b}$ is delayed and the combined output-signal intensity is enhanced to approach the average value resulting from constructive interference with reference signal $\hat{d}$. Thus, the intensity noise of a coherent-state input signal $\hat{a}$ is suppressed in interferometer output signal $\hat{c}$.

The intensity noise of reference signal $\hat{d}$ may disturb the intensity of output signal $\hat{c}$. In order to avoid this spurious noise, the reflectivity of beam splitter $M_2$ should be as high as possible so that the intensity noise of $\hat{d}$ is rejected by beam splitter $M_2$. Although the intensity noise of output signal $\hat{c}$ can be thus suppressed, its phase noise is enhanced by the self-phase-modulation of signal $\hat{b}$ itself as shown in Fig. 2.

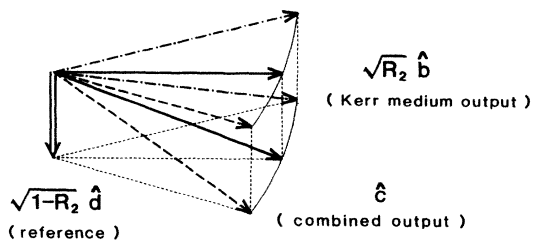


FIG. 2. Principle of photon-number noise reduction by self-phase-modulation and interference; $\Delta \hat{n}_a = 0$ (solid arrows), $\Delta \hat{n}_a > 0$ (dashed-dotted arrows), $\Delta \hat{n}_a < 0$ (dashed arrows).

The goal of our analysis is to demonstrate quantum mechanically that the reduced photon-number noise and enhanced phase noise satisfy the minimum-uncertainty product, i.e., that the output of this nonlinear interferometer is a number-phase minimum-uncertainty state.

If the coupling of the optical field with reservoirs such as optical-loss oscillators and the atomic system of the Kerr medium are adiabatically eliminated, this interferometer can be described as a quantum system with two input ports and two output ports. The input states and output states are connected by the unitary transformation $U$ as

$$|\phi_1\rangle_{\rm in}|\phi_2\rangle_{\rm in}\xrightarrow{U}|\Psi_1\rangle_{\rm out}|\Psi_2\rangle_{\rm out}\ . \tag{2.1}$$

Equivalently, we can express the outputs in terms of two states behind the first beam splitter $M_1$ as

$$|\psi_1\rangle|\psi_2\rangle\xrightarrow{U'}|\Psi_1\rangle_{\rm out}|\Psi_2\rangle_{\rm out}\ . \tag{2.2}$$

If the second beam splitter $M_2$ has sufficiently high reflectivity $R_2\rightarrow 1$, then quantum fluctuations from the reference (lower) arm are not mixed into the output port 1 at $M_2$. Therefore, the contribution of $|\psi_2\rangle$ to $|\Psi_1\rangle_{\rm out}$ is merely a classical driving force, which can be described by an unitary displacement operator

$$D(\xi)=e^{\xi\hat{a}^\dagger-\xi^*\hat{a}} \tag{2.3}$$

as shown in the Appendix. Here, $\hat{a}$ is an annihilation operator of the signal (upper) arm, and the $c$ number $\xi$ indicates the coherent excitation of $|\psi_2\rangle$ measured at output port 1. Therefore, we can describe the output $|\Psi_1\rangle_{\rm out}$ in resolved form as

$$|\Psi_1\rangle_{\rm out}=D(\xi)|\psi_K\rangle\ . \tag{2.4}$$

Since the nonclassical nature of the nonlinear interferometer is entirely due to the optical Kerr effect as shown in Sec. III, the high reflectivity of $M_2$ concentrates the effect into one output $|\Psi_1\rangle_{\rm out}$. If $|\phi_1\rangle_{\rm in}$ is a coherent state and $|\phi_2\rangle_{\rm in}$ a vacuum state, namely,

$$\begin{aligned}|\phi_1\rangle_{\rm in}&=|\alpha_{\rm in}\rangle\ ,\\ |\phi_2\rangle_{\rm in}&=|0\rangle\ ,\end{aligned} \tag{2.5}$$

two coherent states without a quantum-mechanical correlation are prepared behind $M_1$ as

$$\begin{aligned}|\psi_1\rangle&=|\alpha_1\rangle,\ \ \alpha_1=(1-R_1)^{1/2}\alpha_{\rm in}\ ,\\ |\psi_2\rangle&=|\alpha_2\rangle,\ \ \alpha_2=(R_1)^{1/2}\alpha_{\rm in}\ .\end{aligned} \tag{2.6}$$

Here $R_1$ is the reflectivity of $M_1$, and $\alpha_1$ and $\alpha_2$ are $c$ numbers. The state $|\psi_1\rangle$ becomes the nonclassical state $|\psi_K\rangle$ after passage through the Kerr medium, while the state $|\psi_2\rangle$ remains a coherent state $|\alpha_2 e^{i\theta}\rangle$. The high reflectivity of $M_2$ prevents $|\Psi_1\rangle_{\rm out}$ from being contaminated by the state $|\alpha_2 e^{i\theta}\rangle$. As a result of (2.4) and (2.5), the state of output 1 is written as

$$|\Psi_1\rangle_{\rm out}=D(\xi)U_K|\alpha_1\rangle\ . \tag{2.7}$$

Here $U_K$ is a unitary operator connecting input $|\psi_1\rangle$ and output $|\psi_K\rangle$ of the Kerr medium, i.e., representing the self-phase modulation, to be determined in Sec. III. The interference at beam splitter $M_2$ is represented by displacement operator $D(\xi)$. Note that if $\alpha_2$ is sufficiently large, $\xi$ does not vanish even though $R_2\rightarrow 1$. In fact, $\xi$ has a significant role in photon-number noise reduction as discussed in Sec. IV.

## III. SELF-PHASE-MODULATION IN THE KERR MEDIUM

### A. State evolution in the Schrödinger picture

This section investigates the state evolution in the Kerr medium. The optical wave traveling through the Kerr medium is assumed to be plane, polarized, and monochromatic. The traveling wave is treated as a sequence of localized wave packets[30] moving at the speed of $v=c/n_0$, where $n_0$ is the linear refractive index of the Kerr medium and $c$ the speed of light in a vacuum. Each packet has a temporal length of $\tau$ and equivalently a spatial length of $l=\tau v$. Each packet corresponds to a single-mode quantized field written as

$$E(z,t)=i\left[\frac{\hbar\omega_0}{2\epsilon v}\right]^{1/2}\hat{a}(z)e^{i(kz-\omega_0 t)}+\text{H.c.} \tag{3.1}$$

Here $\omega_0$ is angular frequency, $k=\omega_0/v$ is a propagation constant, $\epsilon=n_0^2\epsilon_0$ and $\epsilon_0$ are dielectric constants of the Kerr medium and of a vacuum. $V=Al$ is a quantization volume, where $A$ is a cross-sectional area of the optical beam. The localized annihilation and creation operators $\hat{a}$ and $\hat{a}^\dagger$ obey a commutation relation

$$[\hat{a},\hat{a}^\dagger]=1\ . \tag{3.2}$$

The Hamiltonian for the single-mode electric field in the Kerr medium can be written as[20,33]

$$\begin{aligned}H&=H_0+H_K\ ,\\ H_0&=\hbar\omega_0\hat{a}^\dagger\hat{a}=\hbar\omega_0\hat{n}\ ,\\ H_K&=\hbar\chi(\hat{a}^\dagger)^2\hat{a}^2=\hbar\chi\hat{n}(\hat{n}-1)\ ,\end{aligned} \tag{3.3}$$

in the rotating-wave approximation. The anharmonicity parameter $\chi$ is real and proportional to the third-order nonlinear susceptibility $\chi^{(3)}$ (Ref. 20) or the nonlinear refractive index $n_2$ of the Kerr medium,

$$\chi=\frac{\hbar\omega_0^2 n_2}{2c\epsilon_0 n_0^2 A\tau}\ . \tag{3.4}$$

Here the intensity-dependent refractive index is expressed as[34]

$$n(|\mathscr{E}|^2)=n_0+\tfrac{1}{2}n_2|\mathscr{E}|^2\ , \tag{3.5}$$

where $\mathscr{E}$ is a complex field amplitude defined by $E(z,t)=\frac{1}{2}\mathscr{E}(z,t)e^{i(kz-\omega_0 t)}+\text{c.c.}$ Such a Hamiltonian is valid under the conditions that there is large detuning from transition levels, no saturation, and no loss.[35] Photon number $\hat{n}=\hat{a}^\dagger\hat{a}$ is a constant of motion since

$$[\hat{n},H]=0\ . \tag{3.6}$$

The state evolution during light propagation over a dis-

tance of $z$ in the Kerr medium is expressed as

$$|\psi(z)\rangle = U_K(z)|\psi_1\rangle \ . \tag{3.7}$$

Here $U_K(z)$ is a unitary operator generated by $H_K$ and $|\psi_1\rangle$ is the state at the entrance of the Kerr medium. This is an interaction picture in the sense that the free motion $U_0(z)$ generated by unperturbed Hamiltonian $H_0$ is omitted. However, since $H_K$ commutes with $H_0$, this is equivalent to the Schrödinger picture in the present problem. Therefore we refer to such a state evolution picture as the Schrödinger picture. By replacing the time derivative $\partial/\partial t$ in the Schrödinger equation by the spatial one $-v\partial/\partial z$,[30] the following equation can be obtained for $U_K(z)$:

$$-i\hbar v\frac{dU_K(z)}{dz} = H_K U_K(z) \ , \tag{3.8}$$

where $[H_K, H_0]=0$. The state at the exit of the Kerr medium of length $L$ is written as

$$|\psi_K\rangle = |\psi(L)\rangle = U_K(L)|\psi_1\rangle \ , \tag{3.9}$$

$$U_K(L)=\exp\left[\frac{i}{2}\gamma\hat{n}(\hat{n}-1)\right] , \tag{3.10}$$

where

$$\gamma=\frac{2\chi L}{v}=\frac{\hbar\omega_0^2 n_2 L}{c^2\epsilon_0 n_0 A\tau} \ . \tag{3.11}$$

Such state evolution is clearly represented as a QPD in a complex $\alpha$ plane.[27] We assume the initial state $|\psi_1\rangle$ to be a coherent state $|\alpha_1\rangle$. Then the density operator of the Kerr-medium output state $|\psi_K\rangle$ is written as

$$\rho_K \equiv |\psi_K\rangle\langle\psi_K| = U_K(L)|\alpha_1\rangle\langle\alpha_1|U_K^\dagger(L) \ . \tag{3.12}$$

The QPD, i.e., the "diagonal" matrix element of $\rho_K$ in the coherent-state representation, is

$$\begin{aligned}\bar{\rho}_K^{(n)}(\alpha^*,\alpha) &\equiv \langle\alpha|\rho_K|\alpha\rangle \\ &= |\langle\alpha|\alpha_1\rangle|^2 |\bar{U}_K^{(n)}(\alpha^*,\alpha_1)|^2 \ .\end{aligned} \tag{3.13}$$

Here $\bar{U}_K^{(n)}(\alpha^*,\alpha)$ is an associated normal function[36] of $U_K(\hat{a}^\dagger,\hat{a})$, defined by

$$\bar{U}_K^{(n)}(\alpha^*,\alpha) \equiv \langle\alpha|U_K(\hat{a}^\dagger,\hat{a})|\alpha\rangle \ , \tag{3.14a}$$

in which $\alpha^*$ and $\alpha$ should be regarded as independent variables. Equation (3.13) also uses the relation

$$\langle\alpha|U_K(\hat{a}^\dagger,\hat{a})|\alpha_1\rangle \equiv \langle\alpha|\alpha_1\rangle \bar{U}_K^{(n)}(\alpha^*,\alpha_1) \ . \tag{3.14b}$$

Heffner and Louisell[37] have proposed the normal ordering method which translates the Schrödinger and density-operator equations into $c$-number partial-differential equations for associated normal functions. Yuen[1] has applied this method to obtain the normal ordered form of the unitary operator generated by the quadratic Hamiltonian (1.1). The quadratic Hamiltonian (1.1) is the highest order one solvable in a closed form by the normal ordering method.[38] Our Hamiltonian (1.2) is quartic in $\hat{a}$ and $\hat{a}^\dagger$. On the other hand, the unitary operator (3.10) generated by the quartic Hamiltonian (1.2) is diagonalized on a number basis so that the following series expansion form solution results:

$$\bar{U}_K^{(n)}(\alpha^*,\alpha_1)=e^{-\alpha^*\alpha_1}\sum_{n=0}^{\infty}\frac{(\alpha^*\alpha_1)^n}{n!}e^{(i/2)\gamma n(n-1)} \ . \tag{3.15}$$

Here

$$|\alpha\rangle = e^{-|\alpha|^2/2}\sum_{n=0}^{\infty}\frac{\alpha^n}{\sqrt{n!}}|n\rangle \tag{3.16a}$$

is used.[3] Substituting (3.15) and

$$|\langle\alpha|\alpha_1\rangle|^2 = e^{-|\alpha-\alpha_1|^2} \tag{3.16b}$$

into (3.13), we obtain the following QPD:[29]

$$\begin{aligned}\bar{\rho}_K^{(n)}(\alpha^*,\alpha) &= e^{-(|\alpha|^2+|\alpha_1|^2)} \\ &\times\left|\sum_{n=0}^{\infty}\frac{(\alpha^*\alpha_1)^n}{n!}e^{(i/2)\gamma n(n-1)}\right|^2 \ .\end{aligned} \tag{3.17}$$

We perform numerical calculations for a relatively small photon number $|\alpha_1|^2$ $(=16)$ by terminating the series sum at a sufficiently large $n$ $(=64)$. Since photon-number distribution remains Poissonian with a mean photon number of $|\alpha_1|^2$, termination error is negligible. The results for several $\gamma$ values are shown in Fig. 3. The QPD is represented by the contours of 0.75, 0.5, and 0.25 times the maximum value. The distribution of QPD is expanded in the phase direction while being compressed in the other direction which is slightly different from the photon-number direction. This distribution is deformed analogous to a "crescent" shape from the isotropic distribution of the initial coherent state ($\gamma=0$) as $\gamma$ is increased. This evolution is regarded as a kind of squeezing, but it is essentially different from the "elliptic" squeezing[1,39] of an ordinary squeezed state. However, this difference is not remarkable when the value of $\gamma$ is small. This difference results from the difference in the type of interaction. The former is caused by the four-photon interaction represented by the quartic Hamiltonian (1.2),

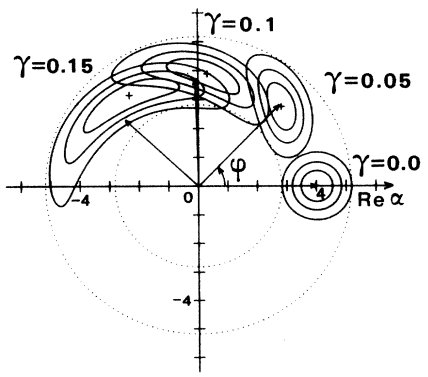


FIG. 3. Quasiprobability density (QPD) $\langle\alpha|\rho_K|\alpha\rangle$ of Kerr-medium output state $|\psi_K\rangle$. $\alpha_1=4.0$, $\gamma=0.0$, 0.05, 0.10, and 0.15. Contours are at 1.0 (+), 0.75, 0.5, and 0.25 times the maximum value. Arrows indicate coherent excitation. $\phi$ is a phase of coherent excitation measured from initial excitation.

while the latter is caused by the two-photon interaction represented by the quadratic Hamiltonian (1.1).

The photon statistics still remain Poissonian at the exit of the Kerr medium,

$$\rho_{K\,nn} \equiv \langle n \mid \rho_K \mid n \rangle = \mid \langle n \mid \alpha_1 \rangle \mid^2 = e^{-\mid \alpha_1 \mid^2} \frac{\mid \alpha_1 \mid^{2n}}{n!} . \tag{3.18}$$

This accounts for the fact that the squeezing direction differs slightly from the photon-number direction in the $\alpha$ plane. However, crescent-shaped squeezing is more appropriate to reduce photon-number noise than the usual elliptic one. This will be shown in Sec. IV.

### B. Operator evolution in the Heisenberg picture

So far, we have worked in the Schrödinger picture to describe the state (or density operator) evolution by the Kerr effect. As discussed in Sec. II, the propagation of optical wave in a Kerr medium is described as a self-phase-modulation in which the phase of optical wave is modulated by its own intensity through the intensity-dependent refractive index (3.5). We will next use the Heisenberg picture to establish an analogy between a phenomenological (or classical) description and a quantum-mechanical description. One advantage of the Heisenberg picture is its ease in being adapted to moment calculation based on the initial coherent state $\mid \alpha_1 \rangle$. The unitary evolution will belong to the operator side,

$$\hat{b} = U_K^{\dagger}(L) \hat{a} U_K(L) , \tag{3.19}$$

where $\hat{a}$ and $\hat{b}$ are annihilation operators for the input and output modes of the Kerr medium. The free motion $e^{i(kz-\omega_0 t)}$ due to unperturbed Hamiltonian is omitted. Using (3.10) and the commutation relation

$$[\hat{a}, \hat{n}] = \hat{a} , \tag{3.20}$$

the output mode operators are described as

$$\hat{b} = e^{i\gamma \hat{n}} \hat{a} , \tag{3.21a}$$

$$\hat{b}^{\dagger} = \hat{a}^{\dagger} e^{-i\gamma \hat{n}} . \tag{3.21b}$$

We can see that the boson commutation relation

$$[\hat{b}, \hat{b}^{\dagger}] = 1 \tag{3.22}$$

is properly preserved after the unitary evolution (3.19). From (3.21a) and (3.21b), we can also see that the photon number is preserved,

$$\hat{b}^{\dagger} \hat{b} = \hat{a}^{\dagger} \hat{a} = \hat{n} . \tag{3.23}$$

The field experiences a phase shift proportional to its photon number. The phase uncertainty is expected to be increased by the photon-number uncertainty of the initial coherent state through such self-phase-modulation. This accounts for the expansion of QPD in the phase direction shown in Fig. 3.

The coherent excitation of the Kerr-medium output field is determined from (3.21a) to be

$$\langle \hat{b} \rangle \equiv \langle \alpha_1 \mid \hat{b} \mid \alpha_1 \rangle = \alpha_1 e^{-\beta/2} e^{i\phi} . \tag{3.24}$$

Here

$$\beta = 4 \mid \alpha_1 \mid^2 \sin^2 \frac{\gamma}{2} , \tag{3.25a}$$

$$\phi = \mid \alpha_1 \mid^2 \sin\gamma . \tag{3.25b}$$

The operator theorem[36]

$$\langle \alpha \mid e^{x \hat{a}^{\dagger} \hat{a}} \mid \alpha \rangle = \exp[(e^x - 1)\alpha^* \alpha] \tag{3.26}$$

is used in the calculation of (3.24). The same coherent excitation of the Kerr-medium output field is also expressed by using the QPD in the Schrödinger picture

$$\bar{\alpha} \equiv \int \alpha \bar{\rho}_K^{(n)}(\alpha^*, \alpha) \frac{d^2\alpha}{\pi}$$

$$= T_r(\rho_K \hat{a}) = \langle \psi_K \mid \hat{a} \mid \psi_K \rangle = \alpha_1 e^{-\beta/2} e^{i\phi} . \tag{3.27}$$

Such coherent excitations are indicated by arrows in Fig. 3.

## IV. REDUCTION OF PHOTON NUMBER UNCERTAINTY BY INTERFERENCE

### A. Photon-number variance evaluation in the Heisenberg picture

This section discusses reduction of photon-number uncertainty by the interference of the Kerr-medium output field with the undisturbed coherent-state field at the second beam splitter $M_2$. First, we work in the Heisenberg picture to calculate the normalized variance of the photon number and to minimize it. Next, we take the Schrödinger picture to describe state and density-operator evolution. Photon-number statistics and QPD after interference are also discussed.

We assume the reflectivity $R_2$ of beam splitter $M_2$ to be sufficiently high as stated in Sec. II. Then, the interference at $M_2$ is written by (2.7) in the Schrödinger picture. For the sake of simplicity, this can be rewritten as

$$\mid \Psi_1 \rangle = D(\xi) U_K(L) \mid \alpha_1 \rangle , \tag{4.1}$$

where $\mid \Psi_1 \rangle_{\text{out}} = \mid \Psi_1 \rangle$. In the Heisenberg picture this interference is expressed as the superposition of the classical field $\xi$ on the Kerr-medium output field $\hat{b}$

$$\hat{c} \equiv U_K^{\dagger}(L) D^{\dagger}(\xi) \hat{a} D(\xi) U_K(L)$$

$$= \hat{b} + \xi = e^{i\gamma \hat{n}} \hat{a} + \xi . \tag{4.2}$$

Here $\hat{c}$ is an annihilation operator of the output mode in port 1. We used Eqs. (3.19) and (3.21a) and a property of the unitary displacement operator

$$D^{\dagger}(\xi) \hat{a} D(\xi) = \hat{a} + \xi . \tag{4.3}$$

The boson commutation relation

$$[\hat{c}, \hat{c}^{\dagger}] = 1 \tag{4.4}$$

is properly preserved after interference (4.2). The photon number of the output mode is written as

$$\hat{n}_c=\hat{c}^{\dagger}\hat{c}=\hat{n}+|\xi|^2+(e^{i\gamma\hat{n}}\hat{a}\xi^*+\text{H.c.}) . \tag{4.5}$$

Here $\hat{n}$ is the photon number of the Kerr-medium input field $\hat{a}$, and the sum in parenthesis is an interference term. This interference term depends on the phase difference of $\hat{b}=e^{i\gamma\hat{n}}\hat{a}$ and $\xi$, which is modulated by $\hat{n}$. Therefore, we can compensate for the fluctuation of $\hat{n}$ with the interference term by an appropriate choice for $\xi$, as discussed in Sec. II.

We seek the $\xi$ which will minimize the photon number uncertainty of output field $\hat{c}$. For this purpose, it is convenient to write $\xi$ as

$$\xi=\eta\alpha_1 e^{i(\phi+\delta)} . \tag{4.6}$$

Here $\eta>0$ is the relative amplitude normalized to the coherent excitation $\alpha_1$ of the initial coherent state and $\delta$ is the phase difference between $\xi$ and $\langle\hat{b}\rangle$. $\phi$ is the phase shift of $\langle\hat{b}\rangle$ due to self-phase modulation and is given by (3.25b). According to the principle stated in Sec. II, the optimum value of $\delta$ is

$$\delta=-\frac{\pi}{2} . \tag{4.7}$$

Thus the mean and variance of the output photon number $\hat{n}_c$ are expressed as

$$\langle\hat{n}_c\rangle\equiv\langle\alpha_1|\hat{n}_c|\alpha_1\rangle=|\alpha_1|^2(1+\eta^2) \tag{4.8}$$

$$\begin{aligned}\langle\Delta\hat{n}_c^2\rangle&=\langle\hat{n}_c\rangle+\langle(\hat{c}^{\dagger})^2\hat{c}^2\rangle-\langle\hat{n}_c\rangle^2\\&=\langle\hat{n}_c\rangle-\langle(\hat{a}^{\dagger})^2\hat{a}^2+4|\xi|^2\hat{a}^{\dagger}\hat{a}+|\xi|^4+2(\xi^*\hat{a}^{\dagger}e^{i\gamma(\hat{n}+1)}\hat{a}^2+\text{H.c.})\\&\quad+(\xi^{*2}e^{i\gamma(2\hat{n}+1)}\hat{a}^2+\text{H.c.})+2|\xi|^2(\xi^*e^{i\gamma\hat{n}}\hat{a}+\text{H.c.})\rangle-\langle\hat{n}_c\rangle^2\\&=\langle\hat{n}_c\rangle-2|\alpha_1|^4\eta\{2e^{-\beta/2}\sin\gamma-\eta[1-e^{-2\beta'}\cos(\gamma-\beta\sin\gamma)]\} ,\end{aligned} \tag{4.9}$$

where Eq. (3.26) is used and

$$\beta'=|\alpha_1|^2\sin^2\gamma . \tag{4.10}$$

The photon-number variance normalized to the mean photon number can then be written as

$$\begin{aligned}\sigma&\equiv\langle\Delta\hat{n}_c^2\rangle/\langle\hat{n}_c\rangle\\&=1-\frac{2\eta(p-q\eta)}{1+\eta^2} ,\end{aligned} \tag{4.11}$$

where

$$p=2|\alpha_1|^2e^{-\beta/2}\sin\gamma , \tag{4.12a}$$

$$q=|\alpha_1|^2[1-e^{-2\beta'}\cos(\gamma-\beta\sin\gamma)] . \tag{4.12b}$$

The normalized variance $\sigma$ defined by the first equality in (4.11) is regarded as a factor which expresses the deviation from the Poisson photon distribution. Namely, $\sigma=1$ corresponds to the Poissonian distribution, $\sigma>1$ to the super-Poissonian, and $\sigma<1$ to the sub-Poissonian. It is also related to the second-order coherence function $g^{(2)}$ measured in the Hanbury Brown–Twiss experiment as

$$g^{(2)}=\frac{\sigma-1}{\langle\hat{n}_c\rangle} . \tag{4.13}$$

Although we assume $\gamma>0$ ($n_2>0$) in the present discussions for the sake of simplicity, the case of having an opposite sign is straightforward. By differentiating (4.11), we obtain the optimum value of $\eta$ for a given $|\alpha_1|^2$ and $\gamma$ as

$$\eta_0=\frac{(p^2+q^2)^{1/2}-q}{p} , \tag{4.14a}$$

which minimizes $\sigma$ to be

$$\sigma_{\min}=1-\frac{2\eta_0(p-q\eta_0)}{1+\eta_0^2} . \tag{4.14b}$$

Examples of numerical calculation for $\sigma_{\min}$ and $\eta_0$ are shown in Fig. 4. According to the numerical results in Fig. 4, the dependence of $\sigma_{\min}$ on $\gamma$ is divided into three regions: (i) a weak squeezing region where $\sigma_{\min}$ is slowly reduced as $\gamma$ increases, (ii) a strong squeezing region where $\sigma_{\min}$ is rapidly reduced in proportion to $\gamma^{-2}$, and (iii) a degraded region where $\sigma_{\min}$ sharply increases in proportion to $\gamma^4$. These three regions are clearly observed in case with a large photon number and are indicated in Figs. 4(c) and 4(d).

When the mean input photon number is large, i.e., $|\alpha_1|^2\gg1$, all of these three regions satisfy $\gamma\ll1$. Approximate expressions can be obtained in this region. If we use

$$\sin\gamma\sim\gamma , \tag{4.15a}$$

$$\beta\sim\beta'\sim\gamma^2|\alpha_1|^2 , \tag{4.15b}$$

$$\phi\sim\gamma|\alpha_1|^2 , \tag{4.15c}$$

instead of the relations in (3.25) and (4.10), the solutions of (4.14) can be simplified as follows ($\beta\ll1$):

$$\sigma_{\min}=1-2\phi[(\phi^2+1)^{1/2}-\phi] , \tag{4.16a}$$

$$\eta_0=(\phi^2+1)^{1/2}-\phi , \tag{4.16b}$$

$$\langle\hat{n}_c\rangle=2|\alpha_1|^2\{1-\phi[(\phi^2+1)^{1/2}-\phi]\} . \tag{4.16c}$$

These are valid in regions (i) and (ii). Moreover ($\beta<1$, $\phi\gg1$),

$$\sigma_{\min}=\frac{1}{4\phi^2}+\frac{1}{6}\beta^2 , \tag{4.17a}$$

$$\eta_0=\frac{1}{2\phi} , \tag{4.17b}$$

$$\langle\hat{n}_c\rangle=|\alpha_1|^2 , \tag{4.17c}$$

are valid in regions (ii) and (iii). The two approximate

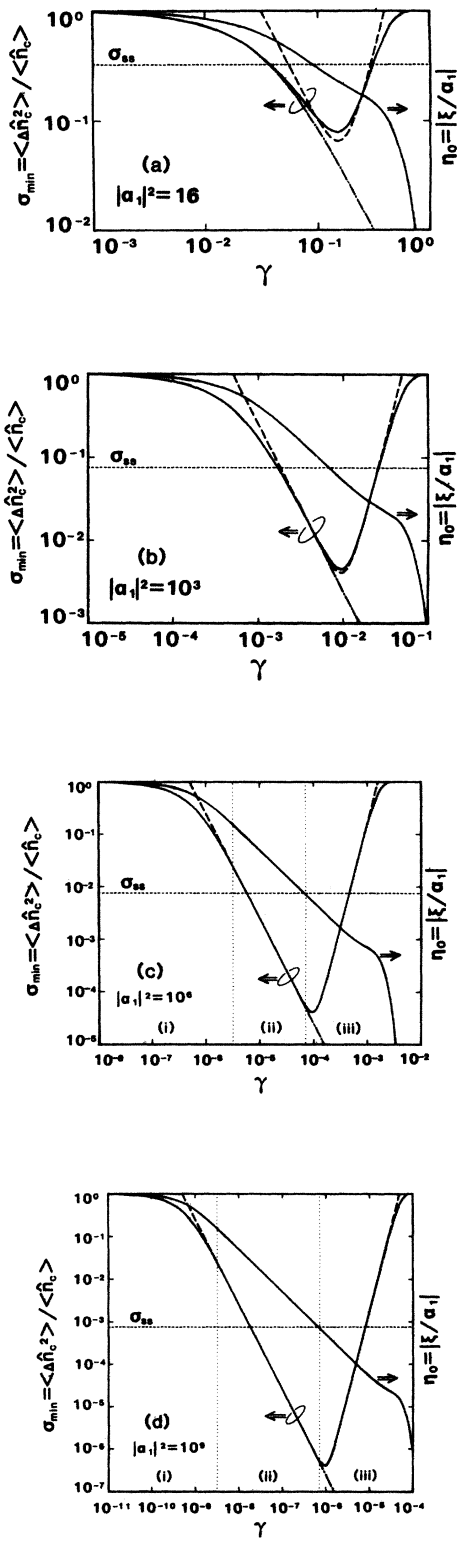


FIG. 4. Minimum photon-number variance $\sigma_{\min}$ and optimum reference wave amplitude $\eta_0$ as a function of $\gamma$. (a) $|\alpha_1|^2=16$, (b) $10^3$, (c) $10^6$, (d) $10^9$. This figure compares exact numerical solution (solid curves), approximate solutions given by (4.16) (dashed-dotted curve) and by (4.17) (dashed curve). The minimum $\sigma_{SS}$ for an ordinary squeezed state is indicated by dotted lines. For regions (i), (ii), and (iii) see text.

solutions (4.16) and (4.17) agree with each other in region (ii) ($\beta\ll 1$ and $\phi\gg 1$), and in good agreement with the exact numerical calculations as shown in Fig. 4. From Fig. 4, $\sigma_{\min}$ takes the minimum in the transit region between (ii) and (iii). This restriction on the reduction in $\sigma_{\min}$ is due to the increase of $\beta$ in (4.17a). The absolute minimum of $\sigma_{\min}$ is determined from (4.17a) and (4.17c) to be

$$\sigma_{\text{abs}}=\left[\frac{3}{4}\right]^{7/6}|\alpha_1|^{-4/3}=\left[\frac{3}{4}\right]^{7/6}\langle\hat{n}_c\rangle^{-2/3}, \quad (4.18)$$

where

$$\gamma_{\text{abs}}=\left[\frac{3}{4}\right]^{1/6}|\alpha_1|^{-4/3}=\left[\frac{3}{4}\right]^{1/6}\langle\hat{n}_c\rangle^{-2/3} \quad (4.19)$$

and

$$\eta_{\text{abs}}=\frac{1}{2}\left[\frac{4}{3}\right]^{1/6}|\alpha_1|^{-2/3}=\frac{1}{2}\left[\frac{4}{3}\right]^{1/6}\langle\hat{n}_c\rangle^{-1/3}. \quad (4.20)$$

According to (4.18a) photon-number variance can be reduced to

$$\langle\Delta\hat{n}_c^{\,2}\rangle_{\text{abs}}=\left[\frac{3}{4}\right]^{7/6}\langle\hat{n}_c\rangle^{1/3}<\langle\hat{n}_c\rangle^{1/3}. \quad (4.21)$$

Note that this is far below the limit $\langle\hat{n}\rangle^{2/3}$ which is the minimum variance achieved by an ordinary squeezed state.[18]

### B. Photon-number statistics and QPD in the Schrödinger picture

Next we investigate the photon-number statistics and QPD of the output state $|\Psi_1\rangle$ in the Schrödinger picture. The density operator of $|\Psi_1\rangle$ is

$$\rho\equiv|\Psi_1\rangle\langle\Psi_1|=D(\xi)\rho_K D^\dagger(\xi)$$
$$=D(\xi)U_K(L)|\alpha_1\rangle\langle\alpha_1|U_K^\dagger(L)D^\dagger(\xi), \quad (4.22)$$

where $\xi$ is given by (4.6), (4.7), and (4.14a). The photon-number distribution is expressed by diagonal matrix elements on a number basis,

$$\rho_{nn}\equiv\langle n|\rho|n\rangle=|\langle n|\Psi_1\rangle|^2. \quad (4.23)$$

Using the following two expressions,

$$D(\xi)=e^{-(1/2)|\xi|^2}e^{\xi\hat{a}^\dagger}e^{-\xi^*\hat{a}}$$
$$=e^{-(1/2)|\xi|^2}\sum_{k=0}^{\infty}\frac{(\xi\hat{a}^\dagger)^k}{k!}\sum_{m=0}^{\infty}\frac{(-\xi^*\hat{a})^m}{m!}, \quad (4.24a)$$

$$\langle n|(\hat{a}^\dagger)^k\hat{a}^m=\begin{cases}0 & (k>n)\\ \dfrac{\sqrt{n!(n-k+m)!}}{(n-k)!}\langle n-k+m| & (k\le n)\end{cases} \quad (4.24b)$$

and series expansion form (3.16a) of $|\alpha_1\rangle$, we can obtain wave function $\langle n|\Psi_1\rangle=\langle n|D(\xi)U_K(L)|\alpha_1\rangle$. Then $\rho_{nn}$

can be expressed as

$$\rho_{nn}=e^{-(|\alpha_1|^2+|\xi|^2)} \times\frac{1}{n!}\left|\sum_{k=0}^{n}\sum_{m=0}^{\infty}\frac{n!\xi^k(-\xi^*)^m\alpha_1^{n-k+m}}{k!m!(n-k)!}\times e^{(i/2)\gamma(n-k+m)(n-k+m-1)}\right|^2 . \tag{4.25}$$

Photon-number distributions can be numerically calculated using this expression. Numerical examples where mean photon numbers are kept constant [$|\alpha_1|^2(1+\eta^2)=16$] for all distributions are shown in Fig. 5(a). The narrowest distribution is for the $\gamma$ value chosen to minimize variance $\langle\Delta\hat{n}_c^2\rangle$ with $\langle\hat{n}_c\rangle$ as a constant. The others are with the two-thirds and one-third $\gamma$ value. Numerical examples in Fig. 5(b) are for an ordinary squeezed state[1] $|\beta_0;\mu,\nu\rangle$ with minimum photon-number variance, and for the coherent state $|\alpha_0\rangle$. Both of these have the same mean photon numbers, which are depicted for comparison. The states $|\Psi_1\rangle$ exhibit strong sub-Poissonian statistics even when the mean photon number is relatively small.

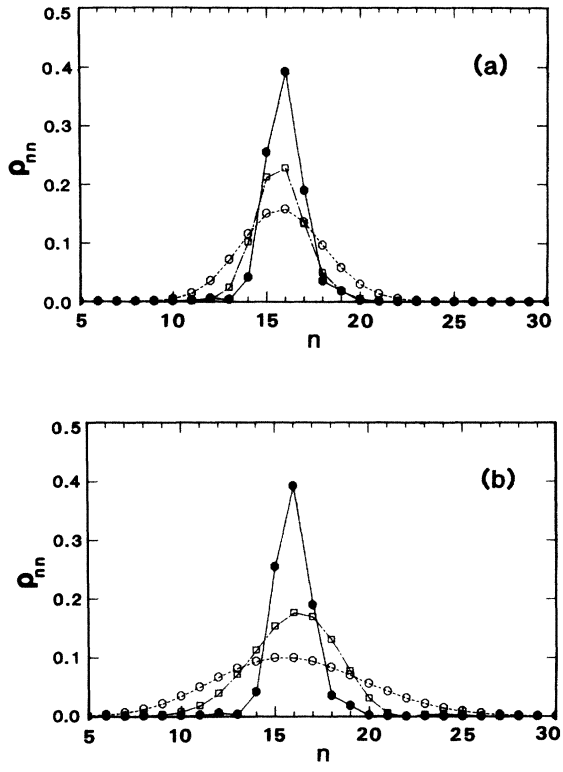


FIG. 5. Photon-number distributions $\rho_{nn}=\langle n|\rho|n\rangle$. (a) $|\Psi_1\rangle$ with $\gamma=0.15$ (●), 0.1 (□), and 0.05 (○); (b) $|\Psi_1\rangle$ with $\gamma=0.15$ (●), ordinary squeezed state $|\beta_0;\mu,\nu\rangle$ with $\nu=0.8$ which minimizes photon-number variance (□), coherent state $|\alpha_0\rangle$ with $\alpha_0=4.0$ (○). Mean photon number is $\langle\hat{n}\rangle=16$ for all states.

Next, we will consider the QPD of the state. The QPD of $|\Psi_1\rangle$, given by the coherent diagonal element of (4.22), is

$$\begin{aligned}\bar{\rho}^{(n)}(\alpha^*,\alpha)&\equiv\langle\alpha|\rho|\alpha\rangle\\&=\langle\alpha|D(\xi)\rho_K D^\dagger(\xi)|\alpha\rangle\\&=\langle\alpha-\xi|\rho_K|\alpha-\xi\rangle ,\end{aligned}\tag{4.26}$$

Here we used

$$D^\dagger(\xi)|\alpha\rangle=D(-\xi)|\alpha\rangle=|\alpha-\xi\rangle . \tag{4.27}$$

Using the definition in (3.13), this can be rewritten as

$$\bar{\rho}^{(n)}(\alpha^*,\alpha)=\bar{\rho}_K^{(n)}(\alpha^*-\xi^*,\alpha-\xi) , \tag{4.28}$$

which is equivalent to $\bar{\rho}_K^{(n)}(\alpha^*,\alpha)$ simply displaced by $\xi$ in the $\alpha$ plane. A change in QPD before and after interference is depicted in Fig. 6. The effect of interference at $M_2$ on $|\psi_K\rangle$ is merely a displacement of QPD in which the shape of QPD does not change. This is because the second beam splitter with a high reflectivity prevents quantum fluctuation of the coherent state in the other arm from entering into the output mode. However, this displacement changes the direction of squeezing to the direction of the photon number. This fact accounts for the reduction of photon-number uncertainty by interference.

We depict the QPD's for $|\Psi_1\rangle$ in Figs. 7(a)–7(c). The QPD's for an ordinary squeezed state[1] and a coherent state are also depicted in Figs. 7(d) and 7(e) for comparison. A comparison of Figs. 7(a) and 7(d) will clarify the difference in the squeezing direction between $|\Psi_1\rangle$ and an ordinary squeezed state. The former is squeezed in photon number, while the latter is squeezed in quadrature amplitude Re$\alpha$. The QPD's of $|\Psi_1\rangle$ roughly from a crescent shape along a circle with radius $\langle\hat{n}_c\rangle^{1/2}$. This results

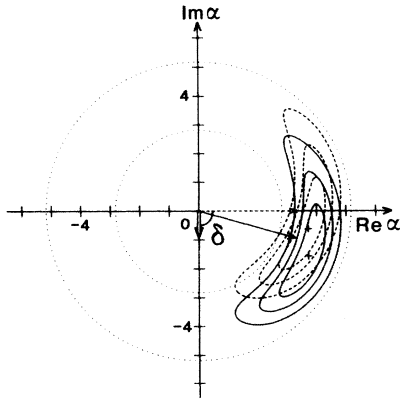


FIG. 6. Displacement of QPD by interference at $M_2$. QPD's are shown by contours at 1.0 (+), 0.75, 0.5, and 0.25 times the maximum value; $|\psi_K\rangle$ before interference (dashed curves), $|\Psi_1\rangle$ after interference (solid curves). Coherent excitations before and after interference are indicated by dashed and solid arrows, respectively. Reference wave is indicated by open arrow. $\gamma=0.15$ and $|\alpha_1|^2(1+\eta^2)=16$.

in strong sub-Poissonian photon statistics in Fig. 5 and extremely reduced photon-number variance. On the other hand, the above described state enhances phase uncertainty more than an ordinary squeezed state. This enhancement of phase uncertainty is treated in Sec. V.

## V. ENHANCED PHASE UNCERTAINTY AND MINIMUM UNCERTAINTY PRODUCT

So far we have shown that the states with reduced photon-number variance are prepared at an output port of the nonlinear interferometer. According to the Heisenberg uncertainty principle, this preparation is only possible with an increased conjugate-variable uncertainty. However, this situation is somewhat more complicated[40] than with cases for other conjugate sets of variables such as position $\hat{q}$ and momentum $\hat{p}$ of a free mass, or two quadrature amplitudes $\hat{a}_1$ and $\hat{a}_2$ for a harmonic oscillator. This is because the Hermitian phase operator $\hat{\Phi}$, which is supposed to be a conjugate variable to photon number $\hat{n}$, does not exist.[41,42] Therefore, we will start with a brief review of phase variables and the number-phase uncertainty relations, according to Susskind and

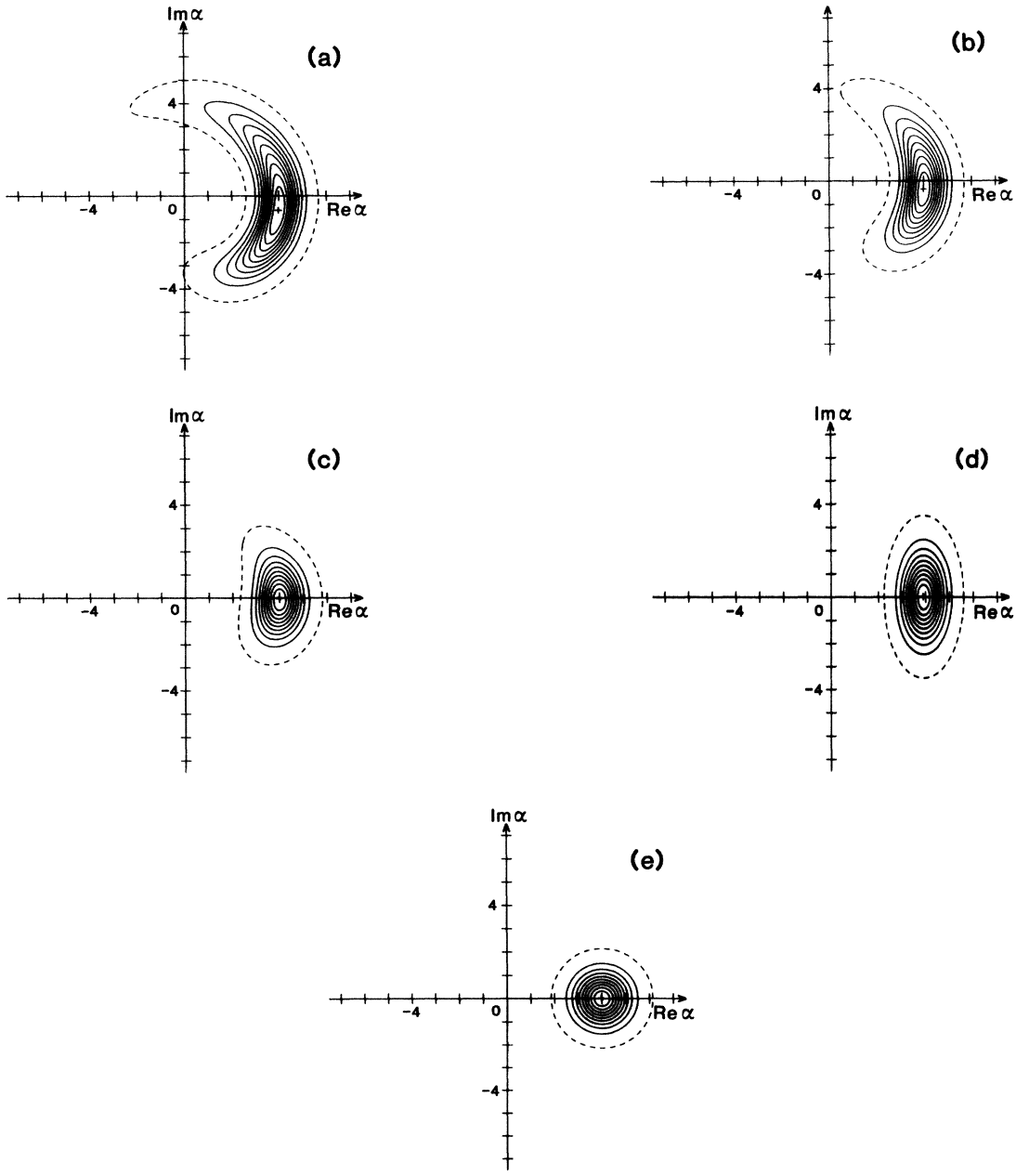


FIG. 7. QPD $\langle \alpha | \rho | \alpha \rangle$ of output state $|\Psi_1\rangle$ with (a) $\gamma=0.15$, (b) $\gamma=0.1$, (c) $\gamma=0.05$, and of (d) ordinary squeezed state $|\beta_0;\mu,\nu\rangle$ with $\nu=0.8$, (e) coherent state $|\alpha_0\rangle$ with $\alpha_0=4.0$. Contours are at 1.0 (+), 0.9, 0.8, . . . , 0.1, and 0.01 (dashed curve) times the maximum value. Mean photon number is $\langle \hat{n} \rangle = 16$ for all states.

Glogower,[41] and Curruthers and Nieto.[31,40] Then we will consider the phase uncertainty and uncertainty product of output state $|\Psi_1\rangle$.

### A. Brief review of number-phase uncertainty relations

Boson annihilation and creation operators $\hat{a}$ and $\hat{a}^\dagger$ are decomposed into photon number $\hat{n}$ and phase factors $\hat{E}_\pm$ as[41,31]

$$\hat{a}=(\hat{n}+1)^{1/2}\hat{E}_- , \tag{5.1a}$$

$$\hat{a}^\dagger=\hat{E}_+(\hat{n}+1)^{1/2} . \tag{5.1b}$$

Inversely, phase factors $\hat{E}_-$ and $\hat{E}_+$ are written as

$$\hat{E}_-=(\hat{n}+1)^{-1/2}\hat{a} , \tag{5.2a}$$

$$\hat{E}_+=\hat{a}^\dagger(\hat{n}+1)^{-1/2} . \tag{5.2b}$$

We cannot adopt the Hermitian phase operator $\hat{\Phi}$ defined by $\hat{E}_-=e^{i\hat{\Phi}}$ and $\hat{E}_+=e^{-i\hat{\Phi}}$, because $\hat{E}_\pm$ are not unitary as shown by[31,41]

$$\hat{E}_+\hat{E}_-=1-|0\rangle\langle 0| \tag{5.3a}$$

even though

$$\hat{E}_-\hat{E}_+=1 . \tag{5.3b}$$

Well-defined Hermitian operators[31,40]

$$\hat{S}=\frac{1}{2i}(\hat{E}_- -\hat{E}_+) , \tag{5.4a}$$

$$\hat{C}=\tfrac{1}{2}(\hat{E}_- +\hat{E}_+) , \tag{5.4b}$$

can be used instead of $\hat{\Phi}$. Their commutation relations are

$$[\hat{n},\hat{S}]=i\hat{C} , \tag{5.5a}$$

$$[\hat{n},\hat{C}]=-i\hat{S} . \tag{5.5b}$$

Heisenberg uncertainty relations directly follow from (5.5) as

$$\langle\Delta\hat{n}^2\rangle\langle\Delta\hat{S}^2\rangle\geq\tfrac{1}{4}\langle\hat{C}\rangle^2 , \tag{5.6a}$$

$$\langle\Delta\hat{n}^2\rangle\langle\Delta\hat{C}^2\rangle\geq\tfrac{1}{4}\langle\hat{S}\rangle^2 . \tag{5.6b}$$

It is more convenient to rewrite them into the following form:[42]

$$P_{nS}\equiv\frac{\langle\Delta\hat{n}^2\rangle\langle\Delta\hat{S}^2\rangle}{\langle\hat{C}\rangle^2}\geq\frac{1}{4} , \tag{5.7a}$$

$$P_{nC}\equiv\frac{\langle\Delta\hat{n}^2\rangle\langle\Delta\hat{C}^2\rangle}{\langle\hat{S}\rangle^2}\geq\frac{1}{4} . \tag{5.7b}$$

Jackiw[32] has mathematically constructed precise minimum-uncertainty states which minimize $P_{nS}$ or $P_{nC}$. He has also shown that no coherent states can minimize them exactly. However, highly excited coherent states are effectively number-phase minimum-uncertainty states. This is because $P_{nS}$ and $P_{nC}$ are very close to the minimum value $\frac{1}{4}$ when their mean photon numbers are sufficiently large, say $\langle\hat{n}\rangle\geq 10$.[31,40]

The expectation values for a coherent state $|\alpha\rangle$, with $\alpha\in R$ and $\alpha^2\gg 1$, are given by[31,40]

$$\langle\alpha|\hat{S}|\alpha\rangle=0 , \tag{5.8a}$$

$$\langle\alpha|\hat{C}|\alpha\rangle\sim 1 , \tag{5.8b}$$

$$\langle\alpha|\Delta\hat{S}^2|\alpha\rangle=\langle\hat{S}^2\rangle\sim\frac{1}{4\alpha^2} . \tag{5.8c}$$

Accordingly, the uncertainty product $P_{nS}$ becomes

$$P_{nS}\sim\tfrac{1}{4} . \tag{5.9}$$

Operators $\hat{E}_\pm$ act on highly excited states as if they were unitary operators since the states are almost orthogonal to the vacuum state $|0\rangle$ in (5.3a). Therefore, we may safely adopt an Hermitian phase operator $\hat{\Phi}$ to write

$$\hat{E}_\pm=e^{\mp i\hat{\Phi}} \tag{5.10}$$

as a good approximation for highly excited coherent states.[43] We may also arbitrarily choose a phase starting point so that

$$\langle\hat{\Phi}\rangle=0 . \tag{5.11}$$

If states are assumed to have a sufficiently small phase uncertainty,

$$\langle\Delta\hat{\Phi}^2\rangle\ll 1 , \tag{5.12}$$

then operators $\hat{S}$ and $\hat{C}$ are well approximated by

$$\hat{S}=\Delta\hat{S}=\Delta\hat{\Phi}-\frac{\Delta\hat{\Phi}^3}{6}+\cdots\sim\Delta\hat{\Phi} , \tag{5.13a}$$

$$\hat{C}=1-\tfrac{1}{2}\Delta\hat{\Phi}^2+\cdots\sim 1 . \tag{5.13b}$$

Accordingly, we treat $\Delta\hat{\Phi}$ and $\Delta\hat{S}$ identically and refer to

$$\langle\Delta\hat{\Phi}^2\rangle\sim\langle\Delta\hat{S}^2\rangle$$

as phase uncertainty. Thus, the commutation relation (5.5a) and the uncertainty relation (5.7a) are reduced to

$$[\hat{n},\hat{\Phi}]\sim i \tag{5.14a}$$

$$P_{n\Phi}\equiv\langle\Delta\hat{n}^2\rangle\langle\Delta\hat{\Phi}^2\rangle\gtrsim\tfrac{1}{4} . \tag{5.14b}$$

We can use the above-mentioned approximate expressions for discussing states with a large mean photon number and small phase uncertainty.

### B. Enhanced phase uncertainty

We turn back to our problem and calculate the change in phase uncertainty in the nonlinear interferometer in the Heisenberg picture. We assume that fields $\hat{a}$, $\hat{b}$, and $\hat{c}$ have large mean photon numbers and small phase uncertainties so that above approximations are safely applicable. Then, the fields are decomposed into the following forms:

$$\hat{a}=(\hat{n}_a+1)^{1/2}e^{i\hat{\Phi}_a} \tag{5.15a}$$

$$\hat{b}=(\hat{n}_b+1)^{1/2}e^{i\hat{\Phi}_b} \tag{5.15b}$$

$$\hat{c}=(\hat{n}_c+1)^{1/2}e^{i\hat{\Phi}_c} . \tag{5.15c}$$

Here Eqs. (5.1a) and (5.10) are used. The number and phase uncertainties of field $\hat{a}$, which is in a coherent state $|\alpha_1\rangle$ with $\alpha_1\in R$ and $\alpha_1^2\gg 1$, are determined from (5.8c) and (5.13a),

$$\langle\Delta\hat{n}_a^2\rangle=\langle\hat{n}_a\rangle=\alpha_1^2 , \tag{5.16a}$$

$$\langle\Delta\hat{\Phi}_a^2\rangle\sim\langle\Delta\hat{S}_a^2\rangle\sim\frac{1}{4\alpha_1^2} . \tag{5.16b}$$

The uncertainty product is very close to the minimum,

$$\langle\Delta\hat{n}_a^2\rangle\langle\Delta\hat{\Phi}_a^2\rangle\sim\tfrac{1}{4} . \tag{5.16c}$$

The phase fluctuation of the Kerr-medium output field $\hat{b}$ is

$$\Delta\hat{\Phi}_b\sim\Delta\hat{\Phi}_a+\gamma\Delta\hat{n}_a\sim\Delta\hat{S}_a+\gamma\Delta\hat{n}_a , \tag{5.17}$$

where (3.20a) and (5.15) are used. The phase uncertainty of $\hat{b}$ is written as

$$\langle\Delta\hat{\Phi}_b^2\rangle\sim\langle\Delta\hat{S}_a^2\rangle+\gamma^2\langle\Delta\hat{n}_a^2\rangle+\gamma\langle\{\Delta\hat{n}_a,\Delta\hat{S}_a\}\rangle , \tag{5.18}$$

where the first two terms are given by (5.16b) and (5.16a). Here the average of the anticommutator $\{\Delta\hat{n}_a,\Delta\hat{S}_a\}=\Delta\hat{n}_a\Delta\hat{S}_a+\Delta\hat{S}_a\Delta\hat{n}_a$ vanishes completely. This is due to the following relation derived using $\alpha_1\in R$:

$$\langle\Delta\hat{n}_a\Delta\hat{S}_a\rangle=\frac{i}{2}\alpha_1\langle(\hat{n}_a+1)^{-1/2}\rangle=-\langle\Delta\hat{S}_a\Delta\hat{n}_a\rangle . \tag{5.19}$$

Phase uncertainty is represented by

$$\langle\Delta\hat{\Phi}_b^2\rangle\sim\frac{1}{4\alpha_1^2}+\gamma^2\langle\hat{n}_a\rangle=\frac{1}{4\alpha_1^2}+\beta , \tag{5.20a}$$

where (4.16) is used. On the other hand, photon-number uncertainty remains constant,

$$\langle\Delta\hat{n}_b^2\rangle=\alpha_1^2 . \tag{5.20b}$$

Therefore uncertainty product is increased to

$$\langle\Delta\hat{n}_b^2\rangle\langle\Delta\hat{\Phi}_b^2\rangle\sim\tfrac{1}{4}+\phi^2 \tag{5.20c}$$

before the interference, where (4.15c) is used.

Next we will consider the phase uncertainty of the output field $\hat{c}$. This will be done by considering cases with varying values for $\phi$. If $\phi\gg 1$ [regions (ii) and (iii) in Fig. 4], the phase uncertainty of $\hat{c}$ is almost the same as that of $\hat{b}$,

$$\langle\Delta\hat{\Phi}_c^2\rangle\simeq\langle\Delta\hat{\Phi}_b^2\rangle\sim\beta\quad(\phi\gg 1) . \tag{5.21a}$$

This is because the superposed field is negligible $\eta_0\ll 1$ as shown by (4.17b). Therefore, using (4.15) and (4.17), the number uncertainty and number-phase uncertainty product are

$$\langle\Delta\hat{n}_c^2\rangle=\alpha_1^2\left[\frac{1}{4\phi^2}+\frac{1}{6}\beta^2\right], \tag{5.21b}$$

$$\langle\Delta\hat{n}_c^2\rangle\langle\Delta\hat{\Phi}_c^2\rangle\sim\tfrac{1}{4}+\tfrac{1}{6}\gamma^6\alpha_1^8 . \tag{5.21c}$$

When the photon-number uncertainty reaches its minimum

$$\langle\Delta\hat{n}_c^2\rangle=\langle\hat{n}_c\rangle^{1/3} \tag{5.22a}$$

at

$$\gamma_1=\tfrac{1}{2}\alpha_1^{-4/3}=\tfrac{1}{2}\langle\hat{n}_c\rangle^{-2/3} , \tag{5.22b}$$

the uncertainty product is still very close to the minimum value

$$\langle\Delta\hat{n}_c^2\rangle\langle\Delta\hat{\Phi}_c^2\rangle\sim\tfrac{1}{4} . \tag{5.22c}$$

This is because the second term of (5.21c) is still negligible (merely 1% contribution).

With a smaller $\phi$ [region (i) in Fig. 4], $\langle\Delta\hat{\Phi}_c^2\rangle$ cannot be directly related to $\langle\Delta\hat{\Phi}_b^2\rangle$, because the superposed field amplitude becomes comparable to the coherent excitation of $\hat{b}$, i.e., $\eta_0\leqq 1$, as shown by Eq. (4.16b). However, the method of quantum-mechanical quasilinearization[44] can be applied to this case. The phases and amplitudes of $\hat{a}$ and $\hat{c}$ can be decomposed into

$$\hat{\Phi}_a=\Phi_a+\Delta\hat{\Phi}_a\quad(\Phi_a\equiv 0) , \tag{5.23a}$$

$$\hat{n}_a^{1/2}=r_a+\Delta\hat{r}_a\quad(r_a\equiv\alpha_1) , \tag{5.23b}$$

$$\hat{\Phi}_c=\Phi_c+\Delta\hat{\Phi}_c , \tag{5.23c}$$

$$\hat{n}_c^{1/2}=r_c+\Delta\hat{r}_c . \tag{5.23d}$$

Here, the first terms are mean values and the second terms are small fluctuations. Then the fields can be expressed as

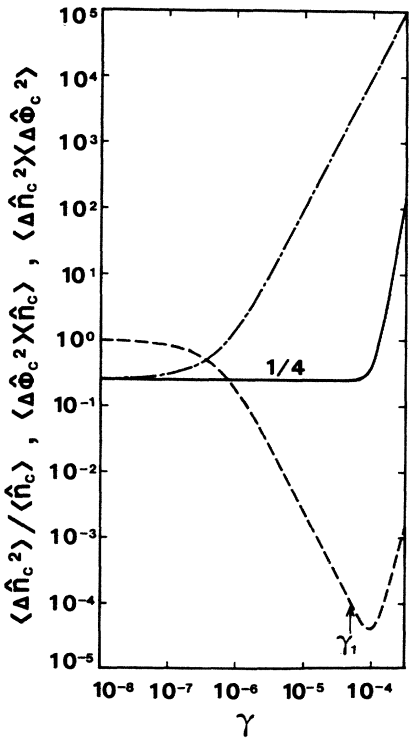


FIG. 8. Number uncertainty (dashed curve), phase uncertainty (dashed-dotted curve) and number-phase uncertainty product (solid curve) of output state $|\Psi_1\rangle$ as a function of $\gamma$. $|\alpha_1|^2=10^6$.

$$\hat{a}=\exp(i\Phi_a)[(r_a+\Delta\hat{r}_a)+ir_a\Delta\hat{\Phi}_a]\ , \tag{5.24a}$$

$$\hat{c}=\exp(i\Phi_c)[(r_c+\Delta\hat{r}_c)+ir_c\Delta\hat{\Phi}_c]\ , \tag{5.24b}$$

where linearization is performed by ignoring the higher-order fluctuation terms. Substituting them into (4.3) with $\xi=-i\eta\alpha_1 e^{i\phi}$, we seek the conditions for minimizing the normalized photon-number variance $\sigma=4\langle\Delta\hat{r}_c^{\,2}\rangle$ and obtain the same results as in (4.16a)–(4.16c). When we choose $\eta=\eta_0\equiv(\phi^2+1)^{1/2}-\phi$, the mean phase of $\hat{c}$ becomes

$$\Phi_c=\phi-\arctan[(\phi^2+1)^{1/2}-\phi]\ . \tag{5.25}$$

Then, phase and number uncertainties and their product can be represented as

$$\langle\Delta\hat{\Phi}_c^{\,2}\rangle=\frac{1}{4\langle\hat{n}_c\rangle[(\phi^2+1)^{1/2}-\phi]^2}\ , \tag{5.26a}$$

$$\langle\Delta\hat{n}_c^{\,2}\rangle=\langle\hat{n}_c\rangle[(\phi^2+1)^{1/2}-\phi]^2\ , \tag{5.26b}$$

$$\langle\Delta\hat{n}_c^{\,2}\rangle\langle\Delta\hat{\Phi}_c^{\,2}\rangle=\tfrac{1}{4}\ , \tag{5.26c}$$

where (5.16a) and (5.16b) are used. These expressions coincide with (5.21) at $\phi\gg1$, as long as the second term of Eq. (5.21c) is negligible, i.e., $\gamma\le\gamma_1$. The results of number and phase uncertainties and the uncertainty product obtained in (5.21) and (5.26) are depicted in Fig. 8.

To conclude this section, the output state of the nonlinear interferometer $|\Psi_1\rangle$ is effectively a number-phase minimum uncertainty state as long as mean photon number is sufficiently large and $\gamma\lesssim\gamma_1$. The photon-number uncertainty can be reduced to $\langle\hat{n}\rangle^{1/3}$.

## VI. NUMBER-PHASE MINIMUM UNCERTAINTY STATE

This section discusses the relation between mathematically constructed number-phase minimum uncertainty states[32] and the output state of the nonlinear interferometer. From general argument of the Heisenberg uncertainty relation,[45] a minimum-uncertainty state of two noncommuting Hermitians $\hat{n}$ and $\hat{S}$ should be the eigenstate of the new operator,

$$\hat{J}_{nS}=\hat{n}+i\zeta\hat{S}\quad(\zeta\in R)\ . \tag{6.1}$$

This is an orthogonally linear combination of the original Hermitians. The eigenvalue equation is given by

$$\hat{J}_{nS}\,|\Psi_{nS}\rangle=(\langle\hat{n}\rangle+i\zeta\langle\hat{S}\rangle)\,|\Psi_{nS}\rangle\ . \tag{6.2}$$

Jackiw[32] has mathematically constructed normalizable states which satisfy this equation with $\langle\hat{S}\rangle=0$. These states are of the form[32,40]

$$|\Psi_{nS}\rangle=\nu\sum_{n=0}^{\infty}I_{n-\lambda}(\zeta)\,|n\rangle \tag{6.3a}$$

with

$$\lambda=\langle\hat{n}\rangle\ , \tag{6.3b}$$

$$\zeta=\left[\frac{\langle\Delta\hat{n}^{\,2}\rangle}{\langle\Delta\hat{S}^{\,2}\rangle}\right]^{1/2}\ , \tag{6.3c}$$

$$I_{-1-\lambda}(\zeta)=0\ , \tag{6.3d}$$

$$|\nu|^2\sum_{n=0}^{\infty}I_{n-\lambda}^2(\zeta)=1\ . \tag{6.3e}$$

Here $I_\mu(\zeta)$ is a modified Bessel function of the first kind of order $\mu$. The parameters $\lambda$ and $\zeta$, respectively, denote the mean photon number and the ratio of number uncertainty to phase uncertainty. They cannot be chosen independently. From the constraint in (6.3d), $\lambda$ must be chosen as $\lambda\in[2k,2k+1]$ ($k=0,1,2,\ldots$) and $\zeta$ ($\ge0$) is uniquely determined by $\lambda$.[46] $\zeta$ is a convex function of $\lambda$ within the range $[2k,2k+1]$, which takes zero at boundaries $\lambda=2k,2k+1$ and takes a maximal value determined by $k$ near the midpoint. Jackiw has excluded photon-number eigenstates ($\lambda=0,1,2,\ldots$; $\zeta=0$) from these states because they do not minimize $P_{nS}$ defined by (5.7).[32]

It would be interesting to test the possibility of making a rigorous number-phase minimum uncertainty state $|\Psi_{nS}\rangle$ from a coherent state or equivalently from a vacuum state through unitary transformation. This can be done as follows. A trivial case $|\Psi_{nS}\rangle=|0\rangle$ is excluded. If the state $|\Psi\rangle$ is generated from a coherent state $|\alpha\rangle$ ($\hat{a}\,|\alpha\rangle=\alpha\,|\alpha\rangle$) through a unitary transformation

$$|\Psi\rangle=U\,|\alpha\rangle\quad(U^\dagger U=UU^\dagger=1)\ , \tag{6.4}$$

then $|\Psi\rangle$ is the eigenstate of the operator

$$\hat{A}=\kappa U\hat{a}U^\dagger\quad(\kappa\neq0)\ , \tag{6.5}$$

with eigenvalue $\kappa\alpha$. Because $[\hat{a},\hat{a}^\dagger]=1$, $\hat{A}$ obeys the commutation relation

$$[\hat{A},\hat{A}^\dagger]=|\kappa|^2\ . \tag{6.6}$$

However, as indicated in (5.5a), $\hat{J}_{nS}$ obeys a completely different commutation relation,

$$[\hat{J}_{nS},\hat{J}_{nS}^\dagger]=2\zeta\hat{C}\ . \tag{6.7}$$

Therefore $|\Psi_{nS}\rangle$ cannot be obtained from a coherent state through a unitary evolution. Of course, no viable physical preparation scheme for $|\Psi_{nS}\rangle$ has yet been proposed.

On the other hand, the output state $|\Psi_1\rangle$ of the nonlinear interferometer is obtained from a coherent state $|\alpha_1\rangle$ through the unitary transformation (4.1). This is physically realized in the nonlinear interferometer. Accordingly, $|\Psi_1\rangle$ cannot be exactly identical to the number-phase minimum-uncertainty state $|\Psi_{nS}\rangle$. However, as long as $\langle\hat{n}\rangle>\langle\Delta\hat{n}^{\,2}\rangle\gtrsim\langle\hat{n}\rangle^{1/3}$, we can generate $|\Psi_1\rangle$ with both $\langle\hat{n}\rangle$ and $\langle\Delta\hat{n}^{\,2}\rangle$ to be exactly equal to those of $|\Psi_{nS}\rangle$ by adjusting $\gamma$, as shown in Sec. IV. As long as $\langle\hat{n}\rangle\gg1$, $\langle\Delta\hat{S}^{\,2}\rangle$ will be almost the same as that of corresponding $|\Psi_{nS}\rangle$. This is because $\langle\Delta\hat{\Phi}^{\,2}\rangle\ll1$ and $\langle\Delta\hat{n}^{\,2}\rangle\langle\Delta\hat{\Phi}^{\,2}\rangle\sim\frac{1}{4}$ are preserved in $|\Psi_1\rangle$. Accordingly, $|\Psi_1\rangle$ is expected to be very close to $|\Psi_{nS}\rangle$. The only difference is that $|\Psi_{nS}\rangle$ maintains mathematical equality in (5.3a) while $|\Psi_1\rangle$ does so only approximately.

The QPD of these two states with the same $\langle\hat{n}\rangle$ and the same $\langle\Delta\hat{n}^{\,2}\rangle=\langle\hat{n}\rangle^{1/3}$ are calculated using (3.15), (4.28), and (6.3a) and are depicted in Fig. 9. They are quite similar even with a relatively small $\langle\hat{n}\rangle$.

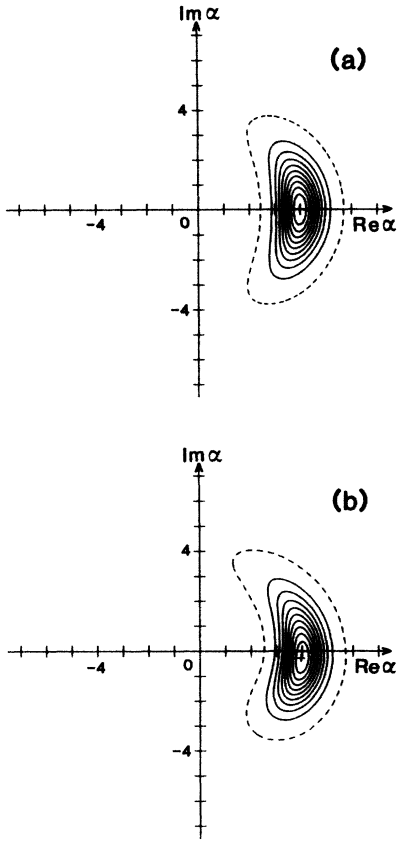


FIG. 9. QPD $\langle\alpha|\rho|\alpha\rangle$ of number-phase minimum uncertainty states; (a) mathematically constructed state $|\Psi_{nS}\rangle$ with $\lambda\sim 16.0$, $\zeta=5.3$, (b) effective minimum-uncertainty state $|\Psi_1\rangle$ with $\gamma=0.0832$. The mean and variance of photon number are $\langle\hat{n}\rangle=16$ and $\langle\Delta\hat{n}^2\rangle=\langle\hat{n}\rangle^{1/3}$ for both states. Contours are at 1.0 (+), 0.9, 0.8, . . . , 0.1, and 0.01 (dashed curve) times the maximum value.

## VII. DISCUSSION

The output state of a nonlinear Mach-Zehnder interferometer has been investigated. The distribution of the quasiprobability density is deformed by self-phase-modulation in a Kerr medium to be a crescent shape. After interference at the high-reflectivity beam splitter, photon-number uncertainty $\langle\Delta\hat{n}^2\rangle$ can be reduced to $\langle\hat{n}\rangle^{1/3}$, far below the limit $\langle\hat{n}\rangle^{2/3}$ for an ordinary squeezed state. The state exhibits strong sub-Poissonian statistics and quasiprobability density squeezed in the direction of the photon number. The reduced number uncertainty and increased phase uncertainty satisfy the Heisenberg uncertainty principle with near equality. The state is effectively a number-phase minimum-uncertainty state.

We have summarized the difference between the state generated by the present scheme and an ordinary squeezed state in Table I. The state discussed here is obtained from a coherent state through unitary transformation $N(\gamma,\xi)=D(\xi)U_K(L)$ which is different from $S(\zeta)$ of an ordinary squeezed state.[4,39] The isotropic QPD of an initial coherent state is squeezed into a crescent shape by $N(\gamma,\xi)$, while it is squeezed into an elliptic shape by $S(\zeta)$ as shown in Fig. 7. The former is more suitable to reduce photon-number uncertainty than the latter. The difference stems from a difference in the type of nonlinear interaction. The former is generated by the four-photon interaction in the signal mode, while the latter by two-photon interaction.

The two-photon interaction necessary for ordinary squeezing is realized in four-photon mixing in a Kerr medium by introducing two strong pump waves in other spatial modes as first proposed by Yuen and Shapiro.[11] However, recent experiments[7,10] employing copropagating four-photon mixing in a Kerr medium seem to deviate from the initial intention in the strict sense and resemble

TABLE I. Effective number-phase minimum-uncertainty state and ordinary squeezed state.

| | Effective number-phase minimum-uncertainty state | Ordinary squeezed state |
|---|---|---|
| Nonlinear interaction | $H_I=\hbar\chi(\hat{a}^\dagger)^2\hat{a}^2$ | $H_I=\hbar[\chi(\hat{a}^\dagger)^2+\chi^*\hat{a}^2]$ |
| Output state | $\|\Psi\rangle_{\text{out}}=N(\gamma,\xi)\|\alpha\rangle$<br>$N(\gamma,\xi)=e^{\xi\hat{a}^\dagger-\xi^*\hat{a}}e^{(i/2)\gamma(\hat{a}^\dagger)^2\hat{a}^2}$ | $\|\Psi\rangle_{\text{out}}=S(\zeta)\|\alpha\rangle$<br>$S(\zeta)=e^{(1/2)\zeta^*\hat{a}^2-(1/2)\zeta(\hat{a}^\dagger)^2}$ |
| Output mode | $\hat{c}=N^\dagger(\gamma,\xi)\hat{a}N(\gamma,\xi)$<br>$=e^{i\gamma\hat{a}^\dagger\hat{a}}\hat{a}+\xi$ | $\hat{b}=S^\dagger(\zeta)\hat{a}S(\zeta)$<br>$=\hat{a}\cosh r-\hat{a}^\dagger e^{i\theta}\sinh r$<br>$(\zeta=re^{i\theta})$ |
| QPD | Crescent | Elliptic |
| Minimum number uncertainty | $\langle\Delta\hat{n}^2\rangle_{\min}=\langle\hat{n}\rangle^{1/3}$ | $\langle\Delta\hat{n}^2\rangle_{\min}=\langle\hat{n}\rangle^{2/3}$ |
| Uncertainty product | $\langle\Delta\hat{n}^2\rangle\langle\Delta\hat{\Phi}^2\rangle\sim\frac{1}{4}$ | $\langle\Delta\hat{a}_1^2\rangle\langle\Delta\hat{a}_2^2\rangle=\frac{1}{16}$ |

our four-photon interaction. Even these copropagating schemes can be well approximated by ordinary squeezing under the following experimental conditions: a small nonlinearity $\phi \sim 1$ and a large photon number $\langle \hat{n} \rangle \gtrsim 10^9$.[47] This is because the quartic Hamiltonian (1.2) is reduced to a quadratic one (1.1) under quasilinearization $\hat{a} = \langle \hat{a} \rangle + \Delta\hat{a}$ with fluctuations higher than those of second order ignored.[28] However, this approximation cannot be extended to cases with an arbitrarily large nonlinearity or a small photon number, since ordinary squeezing generated by quadratic Hamiltonian does not preserve the photon number, though self-phase-modulation (crescent squeezing) generated by quartic Hamiltonian does. Our analysis has revealed the rather encouraging results that such high nonlinearity makes it possible to reduce photon-number uncertainty below the previously known limit.

Frequency domain (multimode) analysis[8] which picks up a coupling between a couple of sideband modes is also linearized and necessarily results in ordinary squeezing. This linearization is justified with a small nonlinearity and a large photon number. However, the extension of the frequency-domain analysis to cases with a large nonlinearity or a small photon number has not yet been developed. Just as for an angular modulated wave with a large modulation index, an infinite number of sideband modes coupled together are required to describe self-phase-modulation properly in the frequency domain.

Recent calculation of the channel-capacity dependence on photon states[48,49] reveal that photon-number eigenstates are far better than ordinary squeezed states in optical communications. The amplitude squeezed state (or effective number-phase minimum-uncertainty state) generated by the present schemes may find important applications in various optical systems.

Although the reduction in photon-number variance is limited by $\langle \hat{n} \rangle^{1/3}$ in the present scheme, further reduction may be achieved by a cascaded configuration of a nonlinear interferometer. This will be treated in a future publication.

## ACKNOWLEDGMENTS

The authors wish to thank N. Imoto, M. Kumagai, and K. Watanabe of NTT Electrical Communications Laboratories for useful discussions. They are also indebted to Dr. H. Kanbe, Dr. F. Kanaya, and Dr. K. Kubodera for their encouragement.

## APPENDIX: INTERFERENCE AT A HIGH REFLECTIVITY MIRROR

We show that interference at beam splitter $M_2$ is expressed by unitary displacement operator for $\hat{b}$ or $\hat{a}$ modes when the reflectivity of $M_2$ is $R_2 \to 1$.

The combined output mode $\hat{c}$ is written as

$$\hat{c} = \sqrt{R_2}\hat{b} + \sqrt{1-R_2}\hat{d} , \tag{A1}$$

where $\hat{b}$ is the Kerr-medium output mode and $\hat{d}$ is the reference arm mode. The reference arm mode can be decomposed into mean and quadrature fluctuations as

$$\hat{d} = \langle \hat{d} \rangle + \Delta\hat{d}_1 + i\Delta\hat{d}_2 . \tag{A2}$$

Since $\hat{d}$ is in a coherent state $|\alpha_2 e^{i\theta}\rangle$,

$$|\langle \hat{d} \rangle| = |\alpha_2| , \tag{A3a}$$

$$\langle \Delta\hat{d}_1^{\,2} \rangle^{1/2} = \langle \Delta\hat{d}_2^{\,2} \rangle^{1/2} = \tfrac{1}{2} . \tag{A3b}$$

If $\hat{d}$ is highly excited, i.e., $|\alpha_2| \gg 1$, then we can let $R_2 \to 1$ while retaining

$$\sqrt{1-R_2}\langle \hat{d} \rangle = \xi , \tag{A4a}$$

where $\xi$ is a $c$ number. However,

$$\sqrt{1-R_2}\Delta\hat{d}_i \to 0 . \tag{A4b}$$

Accordingly, (A1) becomes

$$\hat{c} = \hat{b} + \xi . \tag{A5}$$

The boson commutation relation is properly preserved as

$$[\hat{c}, \hat{c}^\dagger] = [\hat{b}, \hat{b}^\dagger] = 1 . \tag{A6}$$

Using the unitary displacement operator for the $\hat{b}$ mode,

$$D_b(\xi) = e^{\xi\hat{b}^\dagger - \xi^*\hat{b}} . \tag{A7}$$

Equation (A5) can be written as

$$\hat{c} = D_b^\dagger(\xi)\hat{b}D_b(\xi) . \tag{A8}$$

In terms of $\hat{a}$, it is expressed as

$$\hat{c} = U_K^\dagger(L)D^\dagger(\xi)\hat{a}D(\xi)U_K(L) , \tag{A9}$$

where (3.19) is used and

$$D(\xi) = e^{\xi\hat{a}^\dagger - \xi^*\hat{a}} \tag{A10}$$

is the unitary displacement operator for the $\hat{a}$ mode.

In the Schrödinger picture, the output state $|\Psi_1\rangle_{\text{out}}$ is connected to the Kerr-medium input state $|\alpha_1\rangle$ and output state $|\psi_K\rangle$ as

$$|\Psi_1\rangle_{\text{out}} = D(\xi)U_K(L)|\alpha_1\rangle = D(\xi)|\psi_K\rangle , \tag{A11}$$

where (3.9) is used.

[1]H. P. Yuen, Phys. Rev. A 13, 2226 (1976).
[2]D. F. Walls, Nature (London) 306, 141 (1983).
[3]R. J. Glauber, Phys. Rev. 131, 2766 (1963).
[4]D. Stoler, Phys. Rev. D 1, 3217 (1970); 4, 1925 (1971).
[5]R. S. Bondurant, P. Kumar, J. H. Shapiro, and M. Maeda, Phys. Rev. A 30, 343 (1984).
[6]R. E. Slusher *et al.*, Phys. Rev. A 31, 3512 (1985).
[7]M. D. Levenson *et al.*, Phys. Rev. A 32, 1550 (1985).
[8]M. D. Levenson, R. M. Shelby, and S. H. Perlmutter, Opt. Lett. 10, 514 (1985).
[9]R. E. Slusher *et al.*, Phys. Rev. Lett. 55, 2409 (1985).
[10]M. Maeda, P. Kumar, and J. H. Shapiro, Phys. Rev. A 32, 3803 (1985).
[11]H. P. Yuen and J. H. Shapiro, Opt. Lett. 4, 334 (1979).

[12]B. Yurke, Phys. Rev. A **29**, 408 (1984).
[13]P. Kumar and J. H. Shapiro, Phys. Rev. A **30**, 1568 (1984).
[14]M. D. Reid and D. F. Walls, Phys. Rev. A **31**, 1622 (1985).
[15]B. Yurke, Phys. Rev. A **32**, 300 (1985).
[16]Y. Yamamoto, N. Imoto, and S. Machida, Phys. Rev. A **33**, 3243 (1986).
[17]W. Heitler, *Quantum Theory of Radiation* (Oxford University Press, London, 1954), p. 65.
[18]R. S. Bondurant and J. H. Shapiro, Phys. Rev. A **30**, 2548 (1984).
[19]S. Machida and Y. Yamamoto, Opt. Commun. **57**, 290 (1986).
[20]N. Imoto, H. A. Haus, and Y. Yamamoto, Phys. Rev. A **32**, 2287 (1985).
[21]B. E. A. Saleh and M. C. Teich, Opt. Commun. **52**, 429 (1985).
[22]E. Jakeman and J. G. Walker, Opt. Commun. **55**, 219 (1985).
[23]H. A. Haus and Y. Yamamoto, Phys. Rev. A **34**, 270 (1986).
[24]J. H. Shapiro *et al.*, Phys. Rev. Lett. **56**, 1136 (1986).
[25]H. P. Yuen, Phys. Rev. Lett. **20**, 2176 (1986).
[26]H. H. Ritze and A. Bandilla, Opt. Commun. **29**, 126 (1979).
[27]R. J. Glauber, in *Quantum Optics and Electronics,* edited by C. M. DeWitt *et al.* (Gordon and Breach, New York, 1965), p. 138.
[28]P. Tombesi and H. P. Yuen, in *Coherence and Quantum Optics,* edited by L. Mandel and E. Wolf (Plenum, New York, 1984), Vol. V, p. 751.
[29]Dynamics of QPD and quadrature amplitude variances under quartic Hamiltonian (1.2) have been discussed in G. J. Milburn, Phys. Rev. A **33**, p. 674 (1986). However, the QPD's mentioned in his article are for cases with an extremely large nonlinearity ($\gamma > 1$) in which recurrences appear.
[30]Y. R. Shen, in *Quantum Optics,* edited by R. J. Glauber (Academic, New York, 1969), p. 489.
[31]P. Carruthers and M. M. Nieto, Phys. Rev. Lett. **14**, 387 (1965).
[32]R. Jackiw, J. Math. Phys. **9**, 339 (1968).
[33]P. D. Drummond and D. F. Walls, J. Phys. A **13**, 725 (1980).
[34]R. H. Stolen and C. Lin, Phys. Rev. A **17**, 1448 (1978).
[35]M. D. Reid and D. F. Walls, Opt. Commun. **50**, 406 (1984).
[36]W. H. Louisell, *Quantum Statistical Properties of Radiation* (Wiley, New York, 1973).
[37]H. Heffner and W. H. Louisell, J. Math. Phys. **6**, 474 (1965).
[38]J. H. Marburger, J. Math. Phys. **7**, 829 (1966).
[39]C. M. Caves, Phys. Rev. D **23**, 1963 (1981).
[40]P. Carruthers and M. M. Nieto, Rev. Mod. Phys. **40**, 411 (1968).
[41]L. Susskind and J. Glogower, Physics (N.Y.) **1**, 49 (1964).
[42]W. H. Louisell, Phys. Lett. **7**, 60 (1963).
[43]H. Haken, *Light and Matter,* Vol. XXV/2c of *Handbuch der Physik* (Springer-Verlag, Berlin, 1970), pp. 85–87.
[44]H. Haken, Ref. 41, pp. 128–129.
[45]A. Messiah, *Quantum Mechanics* (Interscience, New York, 1961), Vol. I.
[46]G. N. Watson, *Theory of Bessell Functions* (Cambridge University Press, 1962), p. 483.
[47]From (3.11) and (4.15c), $\phi=\mu_0\omega_0 n_2 PL/n_0 A$ in terms of power $P$, where $\mu_0=4\pi\times10^{-7}$ H/m. For example, single-mode optical fiber with $n_0=1.5$, $n_2=1.2\times10^{-22}$ (m/V)$^2$, $A=10^{-10}$ m$^2$, and $L=1$ km and optical field with $P=1$ W at wavelength $\lambda=1.5$ $\mu$m result in $\phi=1.3$. $\langle\hat{n}\rangle=P\tau/\hbar\omega_0=7.5\times10^9$ for $\tau=1$ ns.
[48]Y. Yamamoto and H. A. Haus, Rev. Mod. Phys. (to be published).
[49]H. P. Yuen, in Proceedings of the Conference on Information Sciences and Systems, Johns Hopkins University, 1975, p. 171 (unpublished).